phys. stat. sol. (b) 81, 637 (1977)

Subject classification: 13.4; 6; 22.1.2

Institute for the Study of Defects in Solids, Department of Physics, State University of New York at Albany[1])

Vibrational and Electronic Structure of Hydrogen-Related Defects in Silicon Calculated by the Extended Hückel Theory[2])

By

VIJAY A. SINGH, C. WEIGEL, J. W. CORBETT[3]), and L. M. ROTH

Extended Hückel theory calculations are carried out for interstitial hydrogen atoms in silicon model crystals without and with vacancies. The energetically stable positions for the hydrogens appear to be the tetrahedral interstitial site in crystals without vacancies; in the case of vacancies the hydrogens favor positions in the dangling bonds of the vacancies 0.35 bond lengths away from the vacancy nearest neighbors. The vibrational frequencies for all defect types considered are in very close agreement with infrared bands observed after proton irradiation of silicon. The frequencies increase with the number of hydrogens in a vacancy. The hydrogen-related impurity levels are very close to the valence band edge, both above or below.

Rechnungen nach der erweiterten Hückel-Theorie werden für Wasserstoff-Zwischengitteratome in Silizium-Modellkristallen ohne und mit Leerstellen ausgeführt. Die energetisch stabilen Positionen für die Wasserstoffatome erweisen sich als tetraedrische Zwischengitterplätze in Kristallen ohne Leerstellen. Im Falle von Leerstellen bevorzugen die Wasserstoffatome Positionen in den freien Bindungen der Leerstellen, 0,35 Bindungslängen von den nächsten Nachbaratomen der Leerstelle entfernt. Die Schwingungsfrequenzen für alle betrachteten Defektarten liegen sehr nahe bei denen von Infrarotbanden, die nach Protonenbestrahlung von Silizium beobachtet wurden. Die Frequenzen nehmen mit der Anzahl von Wasserstoffatomen in einer Leerstelle zu. Die Defektniveaus, die von den Wasserstoffatomen herrühren, liegen sehr dicht ober- oder unterhalb der Valenzbandkante.

1. Introduction

We present results of theoretical studies of hydrogen-related defects in the silicon lattice. The presence of such defects has been inferred from the appearance of numerous infrared absorption bands between 4.5 and 5.5 μm (corresponding to (3.43 to 4.19) × $\times$ 10^{14} Hz) after proton irradiation of silicon [1, 2]. These bands still await a satisfactory interpretation. Our work is intended to offer some defect models that can account for the infrared bands. Typically, vibrational modes of atomic complexes and their frequencies are treated by theoretical methods which assume certain force constants for various kinds of distortions of an atomic complex; such methods yield no information concerning the electronic states of the system. On the other hand, in theoretical treatments of the electronic structure a fixed nuclear framework is assumed in most cases.

We employ here a method that was originally developed to determine the electronic and geometric structure of organic molecules, i.e. the extended Hückel theory (EHT) [3]. In later work, especially applications to solid state problems, it was shown that EHT is also capable of describing the elastic properties of a system [4]. Thus,

[1]) Albany, New York 12222, USA.

[2]) Supported in part by the Office of Naval Research under Contract No. 00014-75-C-0919 and by National Science Foundation Grant DMR75-18104.

[3]) John Simon Guggenheim Memorial Fellow.

EHT has been used to determine the vibrational frequencies of the Cu_2 molecule [5] and the substitutional nitrogen in diamond [4]. So our approach to the hydrogen-related defects in silicon is not altogether new, but in this work we want to make more extensive use of this area of applicability of EHT than has been the case so far. We feel that such investigations are particularly useful in that both vibrational and electronic aspects of a defect are considered at the same time.

Due to the approximate nature of EHT we cannot expect our results to be exact in an absolute sense. We can, however, expect to obtain semiquantitative results providing the basis for further more detailed discussions of the defect structure and showing trends of certain physical properties in a family of defects.

Because of the exploratory nature of our calculations, we consider only vibrations of the hydrogen atoms, while we keep all silicon atoms fixed at the positions which they would have in a perfect crystal. This can be largely justified by the large mass difference between hydrogen and silicon atoms. A more refined theoretical treatment should, however, incorporate distortions of the silicon atoms as well. This applies especially to defect complexes that contain vacancies since EPR experiments have shown that the neighbor atoms of monovacancies [6] and divacancies [7] form a lower-symmetry environment of the vacated lattice sites.

In Section 2 we give a brief description of EHT. Section 3 contains information about the model silicon clusters that surround the hydrogen defects in order to simulate the actual solid. In Section 4 we present the results for the energetically stable configurations of one or more hydrogen atoms in the silicon lattice with and without vacancies. We thus assume that the hydrogen atom can find an equilibrium position in essentially unperturbed portions of the lattice and in damaged portions as well. Perhaps the simplest damage is a monovacancy: At room temperature, at which the above-mentioned experiments [1, 2] have been carried out, monovacancies have disappeared, while divacancies still exist. We consider therefore both the mono- and divacancy. Section 5 contains the results for the frequencies of vibrations of the hydrogen atoms around their equilibrium positions. Section 6 gives information on defect-related electron states, and our conclusions are presented in Section 7.

2. Theory

We will give a brief review of the extended Hückel theory (EHT) as applied to our calculations. EHT is well known by now and we shall not give an extensive description of it in this paper. The EHT equations for the molecular orbital (MO) energies (E_i) and the MO coefficients ($c_{\nu i}$) have the same form as the more rigorous Hartree-Fock-Roothan equations,

$$\sum_{\nu=1}^{n} (H_{\mu\nu} - E_i S_{\mu\nu})\, c_{\nu i} = 0\,, \qquad \mu = 1, 2, \ldots, n\,. \tag{2.1}$$

The MO φ_i with energy E_i is a linear combination of atomic orbitals (AO) χ_ν, i.e.

$$\varphi_i = \sum_{\nu=1}^{n} c_{\nu i}\chi_\nu\,. \tag{2.2}$$

The atomic basis states used in our calculations (the χ_μ's) are 3s, $3p_x$, $3p_y$, $3p_z$ Slater-type orbitals. The $S_{\mu\nu}$ are overlap elements between AO's

$$S_{\mu\nu} = \langle \chi_\mu \mid \chi_\nu \rangle\,. \tag{2.3}$$

The $H_{\mu\nu}$, the matrix elements of the Hamilton operator, are then approximated in EHT by

$$H_{\mu\nu} = \tfrac{1}{2} K_{\mu\nu}(H_{\mu\mu} + H_{\nu\nu}) S_{\mu\nu} , \qquad \mu \neq \nu , \tag{2.4}$$

$$H_{\mu\mu} = -I_{\mu} . \tag{2.5}$$

I_{μ} is the empirical atomic ionization energy of the atomic Slater-type orbitals used in the calculation. $K_{\mu\nu}$ is an empirical constant.

In addition to the individual energy levels, we calculate the total EHT energy

$$E_{\mathrm{EHT}} = \sum_{i} n_i E_i , \tag{2.6}$$

where n_i is the occupation number of the i-th state. We use E_{EHT} to determine stable configurations and vibrational frequencies.

The set of parameters used in our theory are those which yielded a good electronic band structure [8]. These are: $K_{\mathrm{ss}} = K_{\mathrm{pp}} = 1.75$; $K_{\mathrm{sp}} = 1.313$; $I_{\mu} = -14.83$ eV for the 3s state of silicon; $I_{\mu} = -7.75$ eV for the 3p state of silicon; $I_{\mu} = -13.6$ eV for hydrogen. The Slater exponent for the atomic wave function in silicon is 1.87 for the 3s state and 1.6 for the 3p state. For hydrogen it is 1.2 for the 1s state [9].

It must be remembered that EHT can justifiably be applied only to systems in which the charge density is uniform. This is the case when the electronegativity difference between neighboring ions is not too large. The electronegativity difference between hydrogen and silicon is 0.3 on the Pauling scale and 0.57 on the Sanderson scale and this falls well within the validity range of EHT. EHT gives unreliable results [10] for ionic systems where the electronegativity difference between adjacent atoms exceeds 1.3 on the Pauling scale [11] and 1.0 on the Sanderson scale [12].

The EHT also fails at small internuclear distances; E_{EHT} does not rise at small decreasing distances as much as required by the nuclear repulsion.

3. Models

The basic geometry and symmetry of diamond-type structures has been described in detail in an earlier paper [13]. Table 1 furnishes a concise description of the four models dealt with in this paper.

Table 1

Various model clusters used in our calculations

symbol	model centre	No. of atoms in cluster	No. of levels in valence band	band gap (eV)
T30	tetrahedral site	30	80	2.29
B32	center of bond	32	85	2.05
S35	substitutional site	35	88	2.12
H38	hexagonal site	38	98	2.24

T30, B32, and S35 have been described in connection with earlier work on carbon interstitial in diamond [13]. The H38 cluster has the hexagonal site as its center, with a total of 38 silicon atoms in all.

The band gap for a real silicon crystal is 1.17 eV at 0 K and 1.14 eV at 300 K [14]. Our values are higher (≈ 2.2 eV) because of the finite size of the cluster. It is worth noting that the largest band gap occurs for the T30 cluster (2.29 eV). This is the smallest sized cluster we have used. A similar result, namely that the band gap of

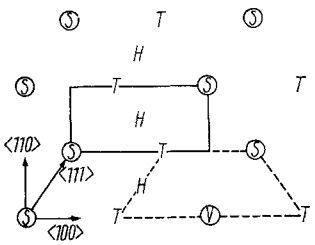

Fig. 1. A portion of a {110} plane of the silicon lattice. The directions of the principle axes are indicated as well as the positions of substitutional lattice atoms (S), tetrahedral (T) and hexagonal (H) interstitial sites. A vacancy (V) is the result of the removal of a lattice atom from an S site. The areas surrounded by solid and dashed lines will be used for the contour maps in Fig. 2 and 3, respectively

model crystals of increasing size decreases eventually towards the actual band structure gap, we obtained for diamond clusters [15].

The T30 and H38 clusters were used to make calculations with hydrogen atoms in an otherwise defect-free silicon crystal. The S35 and B32 clusters were used to make calculations with vacancies. In the S35 cluster, the central substitutional site was removed, thus creating a monovacancy. In the B32 crystal the two central atoms were removed, thus creating a divacancy.

Fig. 1 shows a {110} plane containing all major symmetry and principal crystal axes (also [13]).

4. Stable Configurations

We shall now discuss the stable configuration, migration paths, etc., in each cluster, in detail. The most stable position of the defect hydrogen atom or atoms is one for which the EHT energy E_{EHT} is a minimum.

One H in T30: The central tetrahedral position was found to give a minimum in E_{EHT}. We then plotted the contour map (Fig. 2) as follows: The E_{EHT} energies were calculated for the axes indicated by solid lines. The minimum E_{EHT}, i.e. the value at T was set equal to zero. Symmetry and continuity arguments were also considered. This contour map also indicates that the hexagonal position is a saddle point and that a possible migration path is from one tetrahedral position to another, through the hexagonal.

One and two H in H38: A single hydrogen atom occupying the tetrahedral position close to the center had minimum energy. The central hexagonal position was a saddle

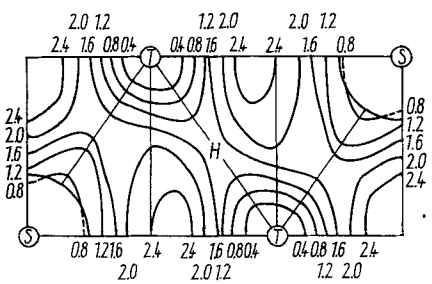

Fig. 2

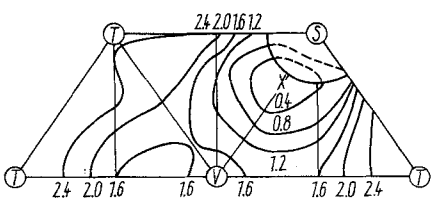

Fig. 3

Fig. 2. E_{EHT} values (eV) of the T30 silicon model clusters as a function of the position of one hydrogen atom placed in the vicinity of the tetrahedral interstitial position (T). The E_{EHT} value at T is set equal to zero. The area of limited validity of EHT (see text) is indicated by the circles around the substitutional lattice sites (S)

Fig. 3. E_{EHT} values (eV) of the S35 silicon model clusters as a function of the position of one hydrogen atom placed in the vicinity of a lattice vacancy (V). The E_{EHT} value at the equilibrium position (X) is set equal to zero. For the circle around S, see caption to Fig. 2

Table 2

Hydrogen positions of E_{EHT} minimum and vibration modes from which the vibration frequencies are calculated. Unless otherwise indicated, the hydrogen atoms are assumed to vibrate along ⟨111⟩ directions (i.e., in the A_1 or A_{1g} modes). Distances are expressed in units of bond length. In the case of more than one hydrogen atom, the position of only one representative atom is given; the positions of the others are determined by the point group symmetry

a) Model cluster without vacancies
T: tetrahedral site, H: hexagonal site

number of hydrogen atoms	model cluster	hydrogen position of E_{EHT} minimum	point group symmetry	vibration mode [16]	vibration frequency (10^{14} Hz)
1	T30	T	T_d	A_1	4.025
1	H38	0.025 from T towards H	C_{3v}	A_1	3.164
2	H38	0.05 from T towards H	D_{3d}	A_{1g}	4.156

b) Model clusters with vacancies
The positions of the hydrogen atoms are given by their distance from the nearest Si atom in the direction towards the nearest vacancy.

number of hydrogen atoms	number of vacancies	model cluster	hydrogen position of E_{EHT} minimum	point group symmetry	vibration mode [16]	vibration frequency (10^{14} Hz)
1	1	S35	0.35	C_{3v}	A_1	3.263
2	1	S35	0.35	C_{2v}	A_1	4.430
3	1	S35	0.35	C_{3v}	A_1	5.547
4	1	S35	0.35	T_d	A_1	6.640
					E*)	5.563
					T_2*)	6.627
6	2	B32	0.35	D_{3d}	A_{1g}	6.390

*) The E and T_2 modes are illustrated in [4]. Here we actually used for T_2 the superposition o the three mutually orthogonal basic T_2 vibrations.

point. The two tetrahedral positions close to the center were found to be the stable positions when two hydrogen atoms were moved symmetrically (breathing mode) away from the central hexagonal position.

One and more H in S35 with vacancy: Extensive calculations were done for one and four hydrogen atoms. The stable positions for one and more hydrogen atoms is indicated in Table 2. It is clear that the hydrogens tend to saturate dangling bonds. The contour map (Fig. 3) for one hydrogen atom reveals that a possible migration path is from one dangling bond to another.

Six H in B32 with divacancy: Six hydrogen atoms were moved in breathing mode fashion from the vacant sites to the nearest neighbors. The results from Table 2 again reveal a tendency towards bond saturation.

Thus, in the case of vacancies, the hydrogen saturates dangling bonds; for no vacancy, it occupies the tetrahedral position.

The circular lines in the contour maps (Fig. 2 and 3) and the dashed broken lines within these circles indicates that EHT grossly underestimates nuclear repulsion in this region. This spurious region is approximately equal to the arithmetic mean of the radii of the silicon and hydrogen atoms [17].

5. Optical Spectra

The stable position for the defects as discussed in the previous section is one with minimum E_{EHT}. When the defect (hydrogen atom) is perturbed from this stable position, we get higher values of E_{EHT}. The perturbation can be expressed in terms of normal coordinates [18]. If the E_{EHT} minimum is taken to be zero, a Taylor expansion in terms of the normal coordinates Q is possible. Thus,

$$\varepsilon = \frac{1}{2} k_2 Q^2 + \frac{1}{6} k_3 Q^3 + \ldots + \frac{1}{n!} k_n Q^n \,. \tag{5.1}$$

Here,

$$\varepsilon = E_{\mathrm{EHT}} - E_{\mathrm{EHT}}^{(\min)} \,. \tag{5.2}$$

Then the frequency of vibration of the defect is

$$\omega = \sqrt{\frac{k_2}{\mu}} \,, \tag{5.3}$$

where

$$\frac{1}{\mu} = d\left(\frac{1}{m_{\mathrm{H}}} + \frac{1}{M_{\mathrm{Si}}}\right) \tag{5.4}$$

with d the number of hydrogen atoms, m_{H} the mass of one hydrogen atom, and M_{Si} the mass of one silicon atom. We displaced the hydrogen atom or atoms about the minimum E_{EHT} position. ε and Q were fitted to a polynomial in (5.1) with $n = 2, 3, 4, 5$, respectively, using a least-squares technique. In obtaining the optimum force constant we took account of several factors. Firstly, we have a finite cluster, so that perturbations made toward the center of the cluster are more reliable. Secondly, in the expansion of (5.1) for $n = 2$, 3, 4, and 5, the value of n for which the root-mean-square deviation is the minimum, is most reliable.

Table 2 lists the frequencies for the various configurations. Some observations of interest are:

Inspite of the approximate nature of EHT, the theoretically calculated frequencies have the same order of magnitude as the experimental values which are comparable to the frequencies of the Si–H bond. This applies to defects with and without vacancies.

In the case of the S35 cluster with the central vacancy, the frequency rises with the increase in the number of hydrogen atoms. This observation was another reason to consider the divacancy with six hydrogen atoms, too. Since this defect complex can be regarded as two vacancies with three hydrogens each, it is not surprising to find its vibrational frequency to be slightly lower that that of the four hydrogens in the vacancy.

For all defects considered, we let the hydrogen atoms vibrate in the appropriate breathing mode. In the case of the central vacancy in the S35 cluster with four hydrogens, we also considered the other possible normal modes, i.e. E and T_2. Their frequencies are lower than that of the breathing mode A_1 distortion, in which the Si–H bonds are only stretched, whereas the bonds can be both bent and stretched in the other modes.

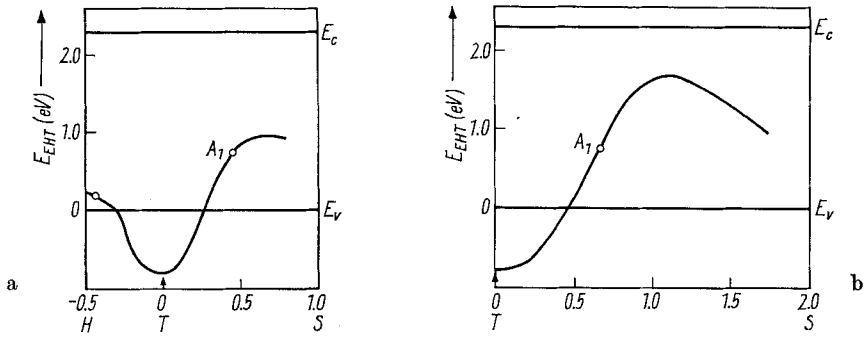

Fig. 4. Energy gap levels for one hydrogen atom moved along a) the ⟨111⟩, and b) the ⟨100⟩ axis from the T-interstitial site of the T30 cluster

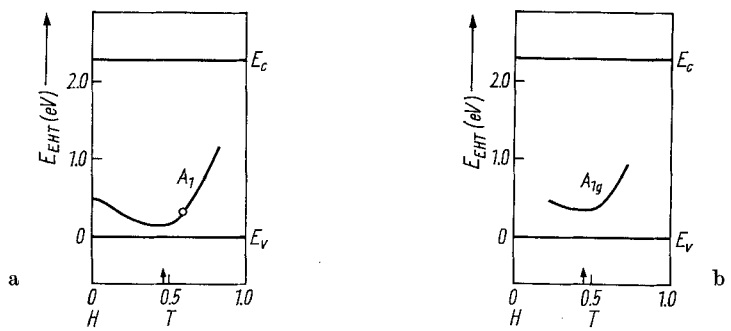

Fig. 5. Energy gap levels for a) one hydrogen atom placed in the ⟨111⟩ axis of the H38 cluster and b) for two hydrogen atoms placed symmetrically with respect to the hexagonal site (H) in the ⟨111⟩ axis of the H38 cluster. In b) the coordinate of only one atom is shown

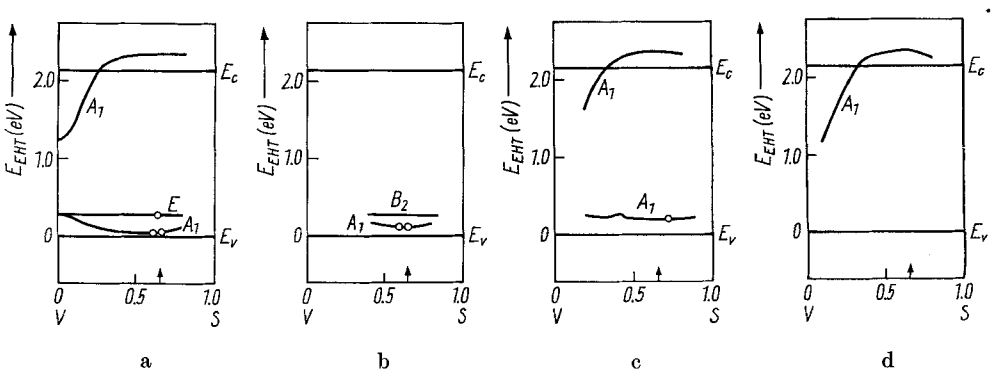

Fig. 6. Energy gap levels for hydrogen atoms placed in the ⟨111⟩ axes of the S35 cluster containing one vacancy (V): a) one hydrogen, b) two, c) three, and d) four hydrogens

Experimentally, a large number of spectral lines have been observed [1, 2]. It should be possible in the near future to identify a few lines and to adjust the limited number of parameters used in the extended Hückel theory to fit these few lines. Once this calibration is made, EHT would be of enormous help in the identification of the rest of the optical spectra due to hydrogen defects in silicon. We are encouraged now to carry on similar studies for other kinds of defects in semiconductors.

6. Electronic States

In Fig. 4 to 7 we have plotted the (one-electron) electronic levels in the vicinity of the energy gap for the systems considered; the energy gaps are indicated by the edges of the valence (E_v) and conduction bands (E_c) as calculated for the model clusters without any defects. The energy levels are plotted as a function of the position of the hydrogen atom; the position corresponding to the minimum E_{EHT} is thereby marked by a vertical arrow on the x-axis.

The occupancy of the energy levels is indicated by solid dots, corresponding to the neutral charge state. The symmetry of the gap states is indicated by the irreducible representation according to which the respective wave function transforms (the corresponding point group is given in Table 1 for each case). With the exception of some vacancy-related states (labeled E in Fig. 6a and B_2 in Fig. 6b), all gap states shown in Fig. 4 to 7 can be called impurity states because in the expansion of their wave function (equation 2.2) the hydrogen 1s stomic state makes a nonvanishing contribution.

Fig. 5 shows a single nondegenerate level is associated with the hydrogen atom in an otherwise defect-free crystal (T30). As the defect vibrates away from the stable position (T), the level will cross the valence band edge and accept a change. This constitutes a one-electron description of a radiationless charge capture and release mechanism. Fig. 6a describes the same situation as Fig. 5a, but now for the larger H38 cluster. Comparing the two we find the same qualitative features, but in the latter, the defect level is still in the band gap. A discrepancy like this can be resolved on surrounding the defect by a very large cluster, thereby eliminating surface effects.

Examining Fig. 5b, we find that the defect state for two hydrogen atoms in an otherwise defect-free crystal has a minimum close to the valence band edge when the hydrogens are located at their respective E_{EHT} minimum positions (T). This observation can be made also for defects involving vacancies (i.e. Fig. 6 a to c with one to three hydrogen atoms in a vacancy and Fig. 7 with six hydrogens in a divacancy). In the case of four hydrogens (Fig. 6d) in a vacancy, this level has been absorbed in the valence band.

We may finally point out that the literature, to our knowledge, reports no experimental information on electronic states that are due to hydrogen impurity atoms

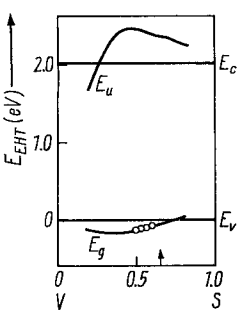

Fig. 7. Energy gap levels for six hydrogen atoms placed in equivalent positions in ⟨111⟩ axes going through the two vacant sites and their six nearest neighbors in the B32 cluster. The coordinate of only one atom is shown

in silicon. Our calculations, which place all hydrogen-related levels very close above or below the valence band edge, give a plausible explanation for this.

We note, however, that shallow donors were electrically observed [19, 20] after proton bombardment of silicon. On the basis of our calculations, which predict deep levels, we must think that these donors are created by the impinging protons but are not related to these simple defects with the hydrogen atoms sitting at their equilibrium positions in the lattice.

Our results concerning the deep hydrogen levels are in marked contrast with experimental [21] and effective-mass-pseudoimpurity theory results [22] for the lithium interstitial in silicon. The lithium also sits at the tetrahedral interstitial site, but is a very shallow donor. The reason for this difference lies probably in the binding of the hydrogen 1s electron to its proton which is much tighter than that of the lithium 2s electron to its nucleus shielded by the 1s core electrons. A similar difference between interstitial hydrogen and lithium concerning their ionizability has already been predicted earlier [23].

One would like to do EHT for lithium and attack at the same time, the more general problem of representing the Rydberg states of such an impurity in an LCAO approach like EHT.

7. Conclusion

Hydrogen is the lightest element and one might be tempted to think that it would move freely in silicon without being tied to a stable position. Nevertheless, as pointed out in Section 4, it tends either to saturate a dangling bond, or occupy the canonical interstitial position, i.e. the tetrahedral position. Our work in Section 5, which deduces frequencies very close to experimentally observed values further confirms the stable configuration of defects. Furthermore, these configurations appear reasonable on simple physical grounds.

Calculations were done for the static lattice. Since hydrogen is such a light atom as compared to silicon we would expect that only minor lattice distortions, if any, will occur. It remains to be seen whether EHT can reliably predict such subtle effects. The relaxations around monovacancies in diamond [4] and divacancies in silicon [24] have, however, been found in EHT calculations to have sizeable values in reasonable agreement with experiments. A more refined treatment should therefore incorporate these relaxations.

Future work in this area would include detection of the existence of an H_2 molecule, a charge consistent calculation to supplement Section 6, calibration and identification of the defect optical spectra, as pointed out towards the end of Section 5, and calculations with other types of defects.

References

[1] H. J. Stein, J. Electron. Mater. **4**, 159 (1975).
[2] N. N. Gerasimenko, L. J. Cheng, Y. H. Lee, J. C. Corelli, and J. W. Corbett, to be published.
[3] R. Hoffmann, J. chem. Phys. **39**, 1397 (1963).
[4] R. P. Messmer and G. D. Watkins, Phys. Rev. B 7, 2568 (1973).
[5] C. R. Hare, T. P. Sleight, W. Cooper, and G. A. Clark, Inorg. Chem. 7, 669 (1968).
[6] G. D. Watkins, J. Phys. Soc. Japan, Suppl. II, **18**, 22 (1963).
[7] G. D. Watkins and J. W. Corbett, Phys. Rev. **138**, A543 (1965).
[8] R. P. Messmer and G. D. Watkins, 1972 (unpublished).
[9] J. A. Pople and G. A. Segal, J. chem. Phys. **43**, S136 (1965).

[10] L. C. ALLEN, in: Sigma Molecular Orbital Theory, Ed. O. SINANOGLU and K. WIBERG, Yale University Press, New Haven 1970 (p. 227).
[11] L. PAULING, in: The Nature of the Chemical Bond, Cornell University Press, Ithaca 1939 (p. 64).
[12] R. T. SANDERSON, in: Chemical Periodicity, Reinhold, New York 1960 (p. 34).
[13] C. WEIGEL, D. PEAK, J. W. CORBETT, G. D. WATKINS, and R. P. MESSMER, Phys. Rev. B 8, 2906 (1973) and references therein.
[14] C. KITTEL, Introduction to Solid State Physics, 4th edition, John Wiley & Sons, Inc., 1971 (p. 364).
[15] R. P. MESSMER and G. D. WATKINS, Phys. Rev. B 7, 2568 (1973).
[16] M. TINKHAM, Group Theory and Quantum Mechanics, McGraw-Hill, New York 1964 (p. 324).
[17] J. C. SLATER, Quantum Theory of Molecules and Solids, Vol. 2, McGraw-Hill, New York 1963 (p. 55).
[18] E. D. WILSON, J. C. DECIUS, and P. C. CROSS, Molecular Vibrations, Chap. 2 and 6, McGraw-Hill, New York 1955.
[19] Y. OHMURA, Y. ZOHTO, and M. KANAZAWA, Solid State Commun. 11, 263 (1972).
[20] YU. V. GORELKINSKII, V. O. SIGLE, and ZH. S. TAKIBAEV, phys. stat. sol. (a) 22, K55 (1974).
[21] R. L. AGGARWAL, P. FISHER, V. MOURZINE, and A. K. RAMDAS, Phys. Rev. 138, A882 (1965).
[22] S. T. PANTELIDES and C. T. SAH, Phys. Rev. B 10, 638 (1974).
[23] H. REISS, J. chem. Phys. 25, 681 (1956).
[24] C. A. J. AMMERLAAN and C. WEIGEL, in: Lattice Defects in Semiconductors 1976, Institute of Physics, London 1977, in the press.

(Received March 25, 1977)